Stability and Control of VTOL Capable Airships in Hovering Flight

H. C. Curtiss Jr.* and V. Sumantran†
Princeton University, Princeton, New Jersey

The stability and control characteristics of an airship equipped with lifting rotors to provide a modest VTOL capability are discussed. The rotors are used for control and maneuvering in near-hovering flight. Configurations with two, three, and four lifting rotors are examined and compared with respect to control capabilities and dynamic response characteristics. Linearized models of the dynamics are employed for this study. A new approach to the prediction of rotor derivatives for operation near zero thrust in hover is presented. It is found that all three configurations have similar control and response characteristics. The responses are characterized by long time constants and low levels of angular damping.

Nomenclature

a = two-dimensional lift curve slope, per radian
C_T = rotor thrust coefficient $= T/[\rho\pi R^2(\Omega R)^2]$
F_B = buoyant force, lb
$I_{xx}, I_{yy}, I_{zz}, I_{xz}$ = vehicle moments of inertia and product of inertia with respect to body axes at center of gravity, slug-ft^2
$I'_{xx}, I'_{yy}, I'_{zz}, I'_{xz}$, = vehicle moments of inertia plus virtual moments of inertia with respect to center of gravity, slug-ft^2
$I'_{xx_{DC}}, I'_{yy_{DC}}, I'_{zz_{DC}}$, = vehicle moments of inertia plus virtual moments of inertia with respect to dynamic center, slug-ft^2
ℓ_T = tail length measured from hull center of buoyancy, ft
M = vehicle mass, slug
M_{AT} = tail surface added mass in Y and Z directions, slug
M_{Ax}, M_{Ay}, M_{Az} = vehicle added mass in X, Y, Z directions, slug
M'_x = $M + M_{Ax}$
M'_y = $M + M_{Ay} + M_{AT} = M + M'_{Ay}$
M'_z = $M + M_{Az} + M_{AT} = M + M'_{Az}$
p, q, r = vehicle angular velocities, rad/s
T, Q = rotor thrust and torque; lb, ft-lb
u, v, w = translational velocities of vehicle center of gravity, ft/s
u_{DC}, v_{DC}, w_{DC} = translational velocities of vehicle dynamic center, ft/s
w_s = vertical velocity of rotor shaft, ft/s
X^*_B = longitudinal distance from center of buoyancy to center of added mass of hull and tail, ft
X_{DC}, Z_{DC} = location of dynamic center with respect to center of gravity for longitudinal motion, ft
X^*_{DC}, Z^*_{DC} = location of dynamic center with respect to center of gravity for lateral-directional motion, ft
Z_A = resultant vertical aerodynamic force in trim, lb
$Z_w, Z_q, M_q, \ldots$ = vehicle stability derivatives normalized by mass and inertia
z_A = Z_A/M'_y
β = buoyancy ratio, $\equiv F_B/Mg$
θ, ϕ = vehicle pitch and roll angles, rad ($p = \dot{\phi}$, $q = \dot{\theta}$)
θ_0 = rotor collective pitch
σ = rotor solidity, ratio of blade area to disk area
$\omega_\theta, \omega_\phi$ = undamped natural frequencies of vehicle in roll and pitch, per second,

$$\omega_\theta^2 = -\frac{1}{I'_{yy_{DC}}}\left.\frac{\partial M}{\partial \theta}\right|_{DC},$$

$$\omega_\phi^2 = -\frac{1}{I'_{xx_{DC}}}\left.\frac{\partial L}{\partial \phi}\right|_{DC}$$

Ω = rotor angular velocity

Introduction

SYSTEM studies conducted over the past 10 years have indicated that lighter-than-air vehicles have the potential to perform a variety of useful and unique tasks.[1-3] Reference 1 indicates that, for maritime patrol, the ability to hover and maneuver near hover is a valuable attribute, essential to many specific mission profiles. This paper is concerned with the examination of the control and stability characteristics of an airship configured to have a modest VTOL capability while retaining the advantages of a conventional airship. While it has been shown that unique hybrid configurations can be designed to produce good control characteristics near hover,[4] this is achieved at the expense of complexity and reduced cruise performance compared to the airship. This investigation was directed toward the examination of relatively conventional airships equipped with tilting rotors such that near hover the rotors could be used for lifting modest payloads as well as maneuvering the vehicle.

Three configurations were examined based on an airship with a nominal volume of 10^6 ft^3 equipped with two, three, and four rotors with a total installed power of 2500 hp.[1] The rotor characteristics were those of the XV-15 tilt-rotor aircraft.[5]

Presented as Paper 83-1987-CP at the AIAA Lighter-Than-Air Systems Conference, Anaheim, Calif., July 25-27, 1983; submitted Sept. 22; revision received Jan. 2, 1985.

*Professor, Department of Mechanical and Aerospace Engineering. Member AIAA.
†Graduate Student, Department of Mechanical and Aerospace Engineering.

Since sophisticated simulations have been developed for this generic-type vehicle,[6,7] the emphasis in this study was placed on the study of a simplified linearized model of the vehicle near hover to provide insight into the important features and limitations of airship control in and near hovering flight. Only the dominant forces and moments produced by the lifting rotors are included in the model. When comparing the resulsts of this investigation to Refs. 7 and 8 it should be noted that both of these studies consider hybrid airships with a heavy-lift capability, while this study investigates the dynamics and control characteristics of a simpler vehicle with smaller lifting rotors and a smaller payload.

Since many proposed hybrid configurations, such as those considered here, may be required to operate in hover with rotor trim thrust values near zero where conventional methods of rotor analysis fail, a new method is presented to estimate the stability derivatives of a rotor operating about this trim state. The equations of motion of the airship are formulated using the dynamic center as a reference point rather than the center of gravity since this permits considerable simplification of the equations of motion. The dynamic center is introduced to eliminate acceleration coupling terms that arise due to the added masses and inertias of the hull.

The control capabilities and dynamic response characteristics of an airship equipped with two, three, and four lifting rotors are examined and compared. The three configurations are referred to in the text as birotor, trirotor, and quadrotor configurations, respectively.

Discussion

The three airship configurations examined in this study are shown in Fig. 1. Control forces and moments are provided through selected combinations of individual rotor cyclic and collective pitch. The rotor rpm is assumed to be perfectly governed and, therefore, constant with respect to the airship body. All three configurations are taken to have the same inertial properties and gross weight as given in the Appendix. The thrust available on each of the three configurations in hover was estimated for 2500 installed horsepower. Table 1 presents maximum values of total thrust, which increases as the number of rotors increases due to a reduction in average disk loading. Based on these results, a maximum payload of 10,000 lb was assumed to provide a suitable power margin for maneuvering. Rotors rotating in both directions are employed such that only the trirotor configuration requires a control to trim unbalanced torque which can be achieved by small amounts of fore and aft cyclic on the forward rotors.

Table 1 Maximum thrust capability of configurations (installed horsepower: 2500)

	Untrimmed, lbs	Trimmed, lbs ($M_{CG}=0$)
Birotor	14,800	14,800
Trirotor	16,900	16,200
Quadrotor	18,600	17,700

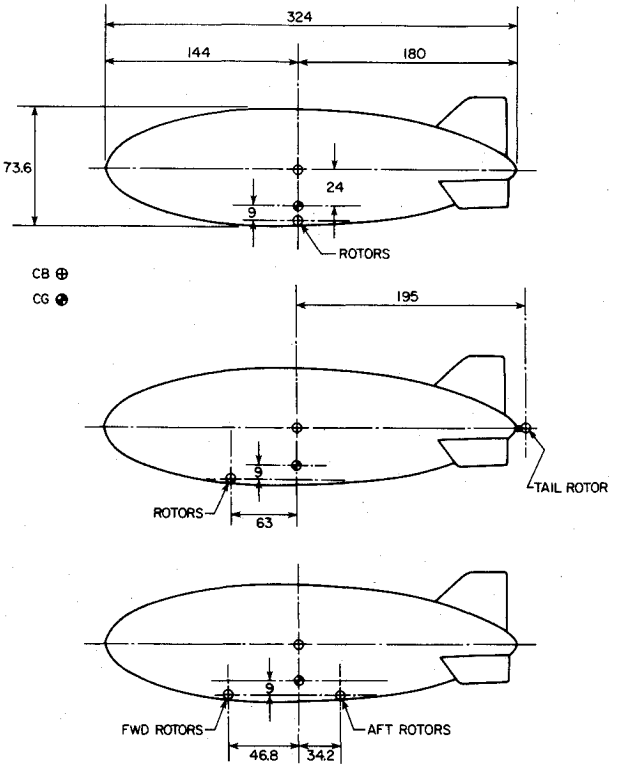

Fig. 1 Configuration geometry. Lateral spacing of rotors: birotor, 88 ft; trirotor, 70 ft; quadrotor, 85 ft.

Equations of Motion

Linearized equations of motion about a steady hovering trim condition are developed using body axes. The linearized equations of motion can be written using the center of gravity as the origin as

$$M\dot{u}=\Delta X \qquad M\dot{v}=\Delta Y \qquad M\dot{w}=\Delta Z \tag{1}$$

$$I_{xx}\dot{p}-I_{xz}\dot{r}=\Delta L \qquad I_{yy}\dot{q}=\Delta M \qquad I_{zz}\dot{r}-I_{xz}\dot{p}=\Delta N$$

The external forces and moments ($\Delta X,\ldots,\Delta N$) arise from 1) gravity, 2) buoyancy, 3) aerodynamic acceleration effects (virtual or added mass), and 4) aerodynamic forces and moments.

Buoyancy and gravity contributions to Eqs. (1) can be expressed for small perturbations about a trim level equilibrium state as follows:

$$\Delta X_{BG}=(F_B-Mg)\theta \qquad \Delta Y_{BG}=-(F_B-Mg)\phi$$

$$\Delta L_{BG}=-F_BZ_B\phi \qquad \Delta M_{BG}=-F_BZ_B\theta$$

$$\Delta N_{BG}=0 \qquad \Delta Z_{BG}=0 \tag{2}$$

It is assumed that the center of gravity (CG) of the vehicle is at the same longitudinal location as the center of buoyancy (CB) as shown in Fig. 1.

The aerodynamic forces and moments that depend upon acceleration are obtained for the hull, assumed to be an ellipsoid of fineness ratio 4.4, from Ref. 9.

The tail contributions to the added mass and moment of inertia are estimated from Ref. 10. An empirical factor of 0.8 is used to account for three-dimensional effects. This contribution should be treated with care to avoid double counting the added mass associated with the hull volume included between the leading and trailing edges of the tail.

Adding buoyancy, gravity, and aerodynamic acceleration terms, the equations of motion become

$$M'_x\dot{u}-M_{Ax}Z_B\dot{q}-(F_B-Mg)\theta=\Delta X_A$$

$$M'_y\dot{v}-M'_{Ay}X^*_B\dot{r}+M'_{Ay}Z_B\dot{p}+(F_B-Mg)\phi=\Delta Y_A$$

$$M'_y\dot{w}+M'_{Ay}X^*_B\dot{q}=\Delta Z_A$$

$$I'_{xx}\dot{p}-I'_{xz}\dot{r}+Z_BM'_{Ay}\dot{v}+F_BZ_B\phi=\Delta L_{CG}$$

$$I'_{yy}\dot{q}-Z_BM_{Ax}\dot{u}+X^*_BM'_{Ay}\dot{w}+F_BZ_B\theta=\Delta M_{CG}$$

$$I'_{zz}\dot{r}-I'_{xz}\dot{p}-X^*_BM'_{Ay}\dot{v}=\Delta N_{CG} \tag{3}$$

The aerodynamic forces and moments due to acceleration result in additional angular and translational acceleration terms in each of the equations. The presence of these terms can be interpreted as associated with an apparent center-of-mass location which is called the dynamic center. Note that since the virtual mass terms are different for motion in the X and Y directions, the dynamic center location is not the same for longitudinal and lateral motions. The dynamic center (DC) location for longitudinal motion is defined as

$$X_{\mathrm{DC}}=\frac{X_B^{*}M_{Ay}'}{M_y'}, \qquad Z_{\mathrm{DC}}=\frac{Z_BM_{Ax}}{M_x'} \tag{4}$$

and for lateral-directional motion,

$$X_{\mathrm{DC}}^{*}=\frac{X_B^{*}M_{Ay}'}{M_y'}, \qquad Z_{\mathrm{DC}}^{*}=\frac{Z_BM_{Ay}'}{M_y'} \tag{5}$$

It may be noted that the fore and aft locations of the dynamic center are the same for both motions. The vertical location of the dynamic center in general will tend to be higher for lateral-directional motions than for longitudinal motion since M_{Ax} is small. Figure 2 shows the location of the dynamic center for the configurations considered here. The equations of motion are transferred to the dynamic center and expressed in terms of the translational velocities of the dynamic center as

$$\begin{aligned}\dot{u}_{\mathrm{DC}}&=\dot{u}-Z_{\mathrm{DC}}\dot{q}\\ \dot{w}_{\mathrm{DC}}&=\dot{w}+X_{\mathrm{DC}}\dot{q}\\ \dot{v}_{\mathrm{DC}}&=\dot{v}-X_{\mathrm{DC}}^{*}\dot{r}+Z_{\mathrm{DC}}^{*}\dot{p}\end{aligned} \tag{6}$$

The equations of motion with respect to the dynamic center are

$$\begin{aligned}M_x'\dot{u}_{\mathrm{DC}}-Z_A\theta&=\Delta X_A\\ M_y'\dot{w}_{\mathrm{DC}}&=\Delta Z_A\\ I_{yy_{\mathrm{DC}}}'\dot{q}-\left.\frac{\partial M}{\partial\theta}\right|_{\mathrm{DC}}\theta&=\Delta M_{\mathrm{DC}}\\ M_y'\dot{v}_{\mathrm{DC}}+Z_A\phi&=\Delta Y_A\\ I_{xx_{\mathrm{DC}}}'\dot{p}-\left.\frac{\partial L}{\partial\phi}\right|_{\mathrm{DC}}\phi&=\Delta L_{\mathrm{DC}}\\ I_{zz_{\mathrm{DC}}}'\dot{r}&=\Delta N_{\mathrm{DC}}\\ q=\dot{\theta}, \qquad p&=\dot{\phi}\end{aligned} \tag{7}$$

Equations (7) now take on a relatively conventional appearance. For simplicity, the small effect of the product of inertia is neglected in the lateral-directional equations. The moments due to buoyancy and gravity have been expressed in terms of effective spring constants

$$\left.\frac{\partial L}{\partial\phi}\right|_{\mathrm{DC}}=-F_B(Z_B-Z_{\mathrm{DC}}^{*}), \qquad \left.\frac{\partial M}{\partial\theta}\right|_{\mathrm{DC}}=-F_B(Z_B-Z_{\mathrm{DC}})$$

The vertical equilibrium relationship has been used to eliminate the buoyancy and gravity terms from horizontal force and side force equations in favor of the resultant aerodynamic force Z_A, i.e.,

$$Z_A=F_B-Mg=(\beta-1)Mg$$

When payload is added to the vehicle it is assumed to be located at the center of gravity of the unloaded vehicle and included in M and, therefore, a sling load is not considered in this study. The relative size of the payload is considerably smaller than that considered in Refs. 7 and 8, therefore, the effects of a sling load on the dynamic characteristics would be of less importance here.

It can be seen from Eqs. (7) that the dynamic center acts similar to the center of mass. That is, a pitching moment acting about the dynamic center produces only angular acceleration and a force applied at the dynamic center produces a translational acceleration of the dynamic center.

The rotor contributions to the equations of motion ($\Delta X_A,\ldots,\Delta N_{\mathrm{DC}}$) are now formulated.

Hull-rotor interference is neglected. While there may be effects of some importance to this investigation, the limited extent and somewhat inconsistent nature of the experimental data[11] have made it difficult to develop a theoretical approach. Reference 6 has considered these effects extensively and shows that the first-order effects are on crosswind performance with little influence on the vehicle dynamics.

The rotor contributions have been modeled in a simplified way assuming that only rotor thrust and torque variations are of importance in the vehicle dynamics, and that the only significant changes in these quantities arise from local vertical velocity variations along the rotor shaft, collective pitch, and shaft angular velocity. Linearized variations of thrust and torque with in-plane velocity are zero in hover. The contribution of the rotor in-plane force produced by pitching velocity is small compared to the thrust variation due to the large rotor spacing and is neglected. Interference between rotors is also neglected because the rotor separation is more than two diameters in all cases.

Rotor hub moments are also neglected. The XV-15 rotor is gimbaled with a very soft hub spring and, consequently, the hub moment can be neglected. Rotor in-plane forces due to cyclic pitch application are included. The effect of the negative δ_3 hinge on the XV-15 rotor is also neglected, since this would act only to reduce the translational force produced by the cyclic pitch.

Consequently, the only rotor derivatives that have been included in the analysis are the rate of change of thrust and torque with collective pitch, vertical velocity along the shaft, and angular velocity,

$$\frac{\partial T}{\partial w_s}, \quad \frac{\partial T}{\partial\theta_0}, \quad \frac{\partial T}{\partial\Omega}, \quad \frac{\partial Q}{\partial w_s}, \quad \frac{\partial Q}{\partial\theta_0}, \quad \frac{\partial Q}{\partial\Omega}$$

where w_s is the local velocity along the rotor shaft induced by vehicle dynamic center motion. The thrust variation with vertical velocity gives rise to pitch and roll damping as well as a pitching moment change with climb velocity due to the location of the rotors. Incorporating these effects gives rise to the complete set of equations of motion,

$$\begin{aligned}\dot{u}_{\mathrm{DC}}-\frac{M_y'}{M_x'}z_A\theta&=\frac{\delta X}{M_x'}\\ \dot{w}_{\mathrm{DC}}-Z_ww_{\mathrm{DC}}-Z_qq&=\frac{\delta Z}{M_y'}\\ \dot{q}-M_qq-M_ww_{\mathrm{DC}}+\omega_\theta^2\theta&=\frac{\delta M_{\mathrm{DC}}}{I_{yy_{\mathrm{DC}}}'}\end{aligned} \tag{8}$$

$$\dot{v}_{DC}+z_A\phi=\frac{\delta Y}{M_y}$$

$$\dot{p}-L_p p+\omega_\phi^2\phi-L_r r=\frac{\delta L_{DC}}{I_{xx_{DC}}}$$

$$\dot{r}-N_r r-N_p p=\frac{\delta N_{DC}}{I_{zz_{DC}}} \tag{9}$$

where the terms on the right-hand side arise from control inputs. These are the equations of motion used in this investigation. The small longitudinal/lateral coupling effects that would be present in the trirotor configuration have been neglected. The rotor derivatives must be evaluated so the total vehicle stability derivatives can be calculated. Of particular interest is the variation of thrust coefficient with vertical velocity and collective pitch. Using blade element and momentum theory,[12] assuming uniform inflow, the rotor thrust coefficient variations are given by

$$\frac{2}{a\sigma}\frac{dC_T}{d\theta_0}=\frac{1/3}{1+(a\sigma/16)\sqrt{2/C_{T_0}}} \tag{10}$$

and

$$\frac{dC_T}{d\bar{w}}=\frac{3}{4}\frac{dC_T}{d\theta_0}$$

It can be seen that conventional rotor theory yields the result that at trim rotor thrust equal to zero, both of these derivatives are equal to zero. There is no control or damping present in a linear sense. A close examination of the assumptions contained in these equations indicates that the annular form of momentum theory should be employed at low thrust coefficients to account for radial variations in the induced velocity. To include the effect of twist on the inflow distribution, the rotor disk is divided into two regions: outboard and inboard of the radial station X_c where the local pitch angle is zero. The twist is assumed to be hyperbolic and the thrust coefficient can be expressed as a function of collective pitch θ_0 and the radial station where the pitch is zero (X_c) as

$$C_T^*=\frac{\hat{\theta}_0}{6}\left[1-\frac{3}{2}X_c\right]+\left[X_c^2-\frac{1}{2}\right]-I \tag{11}$$

where

$$X_c=-\frac{\theta_1}{\theta_0},\qquad C_T^*=\frac{32C_T}{(a\sigma)^2},\qquad \hat{\theta}_0=\frac{32}{a\theta}\theta_0$$

and

$$I=\frac{2}{\hat{\theta}_0^2}\left\{-\frac{4}{15}+\frac{2}{15}[1-\hat{\theta}_0X_c]^{3/2}-\frac{[1+\hat{\theta}_0(X_c-1)]^{5/2}}{5}+\frac{[1+\hat{\theta}_0X_c][1+\hat{\theta}_0(X_c-1)]^{3/2}}{3}\right\}$$

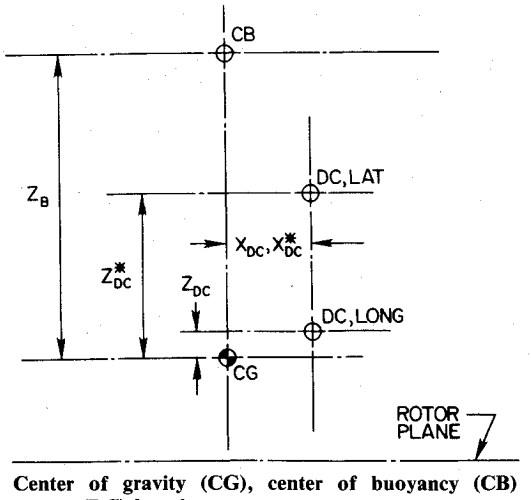

Fig. 2 Center of gravity (CG), center of buoyancy (CB) and dynamic center (DC) locations.

For a given blade twist (θ_1), Eq. (11) is solved for the value of collective pitch that produces zero thrust. Incrementing the rotor collective pitch by a small value, the new value of thrust is determined and the thrust variation with collective pitch is calculated. The variation of thrust coefficient with collective pitch is very sensitive to blade twist (θ_1) near the zero thrust trim condition, as shown in Fig. 3. A similar approach can be used to determine the thrust variation with vertical velocity. For typical values of twist, Fig. 3 shows that the control derivatives decrease by about a factor of 2 as the thrust is reduced from the full payload value to zero thrust. The equivalent hyperbolic twist for the XV-15 rotor is 6.5 deg.

Rotor thrust and rotor torque also vary due to the effect of vehicle yaw rate on the angular velocity of the rotor blades with respect to the air mass. The torque derivatives follow directly from the thrust derivatives.

Control Forces and Moments

Table 2 presents control sensitivity characteristics of the three configurations studied at full payload. It is likely that the most effective means to control these vehicles is through the direct use of translation forces.[4] Use of moments to tilt

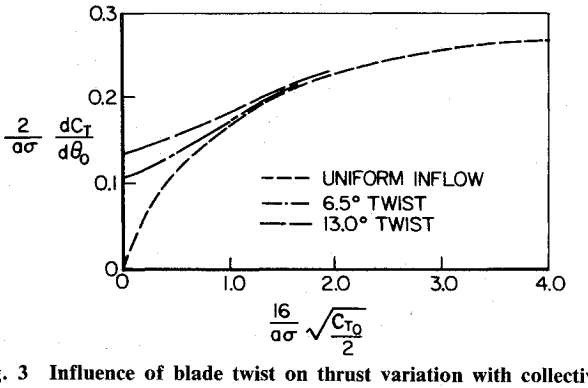

Fig. 3 Influence of blade twist on thrust variation with collective pitch as a function of trim thrust coefficient.

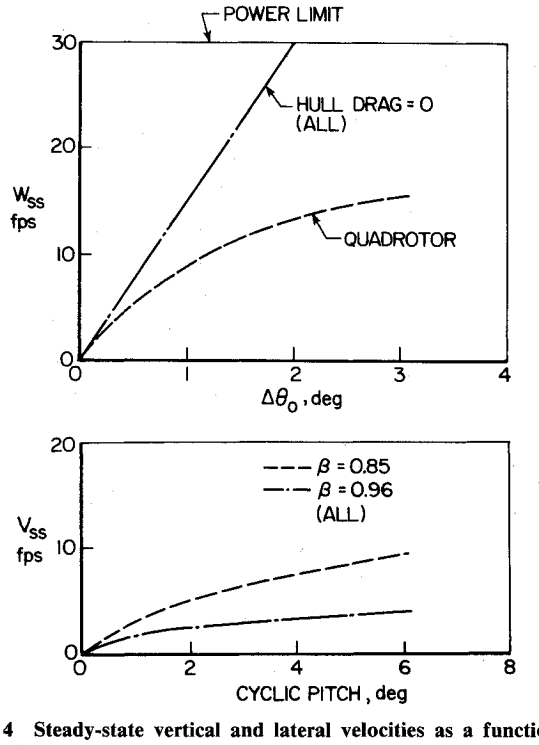

Fig. 4 Steady-state vertical and lateral velocities as a function of collective and cyclic pitch inputs.

the relatively small thrust vector for translation is likely to be an inefficient means of control. Both collective and cyclic inputs produce translational as well as rotational accelerations. It can be seen, however, that the differential collective controls are relatively powerful and, therefore, only a low level of mixing is required to eliminate the pitching and rolling accelerations due to cyclic pitch. Note that the birotor configuration does not have a pitching moment control. Recall that, to eliminate acceleration coupling, the moment about the dynamic center of the vehicle rather than the center of mass should be made equal to zero by control mixing.

As the payload is reduced, the values of these gradients are reduced. The cyclic control effectiveness depends directly on the thrust level and is equal to zero at zero thrust except in the case of the quadrotor. With four lifting rotors, it is possible to obtain control forces with cyclic deflection while maintaining vertical equilibrium by thrusting downward on two opposite rotors. The level that can be achieved in this way depends upon the allowable negative thrust of the rotor employed. Of course, there will be a loss of efficiency in the negative thrust direction due to twist.

The distinguishing features of the three vehicles can be seen to be the fact that the birotor has no pitch control capability, and the quadrotor has the ability to produce lateral and longitudinal forces at zero net thrust.

It is difficult to decide what constitutes a satisfactory control level for this type of vehicle, although some remarks can be made.

The yaw acceleration per degree of cyclic is about equivalent to that which would be obtained from 1 deg of rudder deflection at a flight velocity of 15 knots based on the experimental data of Ref. 13. At full payload, 10 deg of lateral cyclic approximately balances a 6.5-knot steady lateral gust as shown in Fig. 4. At lower payloads (larger buoyancy ratios), the steady lateral velocity that can be balanced is reduced as shown in Fig. 4. Also shown is the vertical trim velocity as a function of collective pitch with and without the influence of hull crosswind drag for the quadrotor configuration.

Some appreciation for the size of the lateral and longitudinal control forces available can be obtained by examining the ratio of acceleration produced by cyclic pitch to that produced by roll or pitch of a helicopter, i.e., a vehicle with a buoyancy ratio of zero. This ratio is $(1-\beta)^{-1}$ in the longitudinal case and approximately $0.5(1-\beta)^{-1}$ in the lateral case due to the larger added mass. At the buoyancy ratio corresponding to a payload of 10,000 lb ($\beta=0.85$) this ratio is about 7, i.e., the application of 10 deg of cyclic produces a translational force equivalent to that produced by tilting a helicopter about 1.4 deg in the longitudinal direction, and about one-half this value in the lateral direction. The vertical acceleration capability is also reduced by a similar factor, i.e., approximately $0.5(1-\beta)$.

The control force capability of these configurations is thus quite limited when compared to a helicopter.

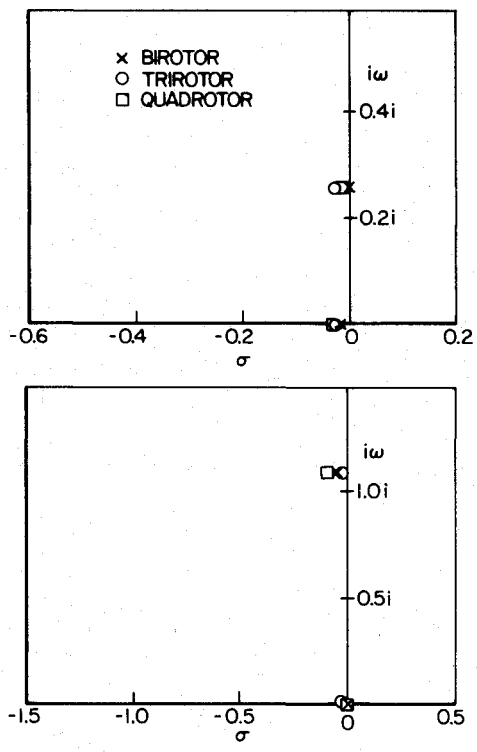

Fig. 5 Characteristic modes of configurations with payload ($\beta=0.85$). Longitudinal and lateral-directional.

Table 2 Control sensitivity

	Birotor	Trirotor	Quadrotor
Longitudinal cyclic pitch[a]			
$\dot{u}_{DC}$	0.08	0.08	0.08
$\dot{q}$	0.005	0.001	0.005
Collective pitch[b]			
$\dot{w}_{DC}$	−0.21	−0.29	−0.37
$\dot{q}$	0.016	−0.042	0.062
Geared collective pitch ($\dot{q}=0$)			
$\dot{w}_{DC}$	—	−0.27 (1 deg, 1deg, 0.73 deg)	−0.28 (0.5 deg, 0.5 deg, 1 deg, 1 deg)
Differential longitudinal collective[b] (no net thrust)			
$\dot{q}$	0	0.29 (0.5 deg, 0.5 deg, −1 deg)	0.18
Lateral cyclic pitch[a]			
$\dot{v}_{DC}$	0.04	0.04	0.04
$\dot{p}$	−0.17	−0.07	−0.017
$\dot{r}$	0.003	0.003	0.003
Differential lateral collective[b]			
$\dot{p}$	1.76	1.34	3.0
Differential cyclic pitch[a]			
$\dot{r}$	0.02	0.036	0.02
$\dot{v}_{DC}$	0	0.01	0

Note: Translational acceleration given in ft/s^2 deg and angular acceleration in deg/s^2/deg

[a]Acceleration proportional to trim thrust. [b]Control sensitivity at zero thrust reduced approximately 50%.

Vehicle Dynamics

As noted in the development, the longitudinal modes of motion are uncoupled from the lateral-directional modes. The eigenvalues of the three vehicles are shown in Fig. 5. The longitudinal dynamics include a lightly damped oscillation with a period of about 24 s and a damping ratio on the order of 0.1 or less for all three configurations. The trirotor vehicle has the largest pitch damping due to rotor spacing which results in a damping ratio of 0.12. Again for comparison purposes, it may be noted that this is about the same level of damping as produced by the fixed tail surfaces at a translational flight speed of 10 knots using the data of Ref. 13.

The heave mode has a moderately long time constant that ranges from 30 s for the quadrotor vehicle to 60 s for the birotor vehicle. This is a considerably larger time constant than shown in Refs. 7 and 8 due to the smaller rotors on the vehicle configurations studied. The remaining characteristic root is at the origin since the translational damping due to rotor in-plane forces has been neglected as noted earlier.

The lateral-directional dynamics include an oscillatory roll-sway mode with a period of about 6 s that is lightly damped. The period is shorter than in the longitudinal case due to the smaller inertia but, as in the longitudinal motion, the lifting rotors are too small to provide any significant level of roll damping. The yaw damping is essentially negligible for all three configurations and, therefore, there is also a pole at the origin.

Recall that the speed stability and dihedral effect that arise from rotor in-plane forces have been neglected. Both of these terms would be slightly unstable in a static sense due to the location of the rotors below the dynamic center. However, it can be shown that the effect of these terms is negligible when compared to the influence of the pitch and roll attitude stability produced by the CB/CG spacing. Thus the characteristic motions are quite different from what would be expected on a hovering helicopter of this size. This simplified model yields an oscillatory mode that forces a small amount of translation due to tilting of the aerodynamic thrust vector proportional to $(1-\beta)g$ and, therefore, with $\beta = 0.85$ this effect is considerably smaller than for a helicopter where $\beta = 0$.

The geometric shape of the oscillatory modes depends upon the buoyancy ratio (aerodynamic thrust) and the metacentric height. For the case where the buoyancy ratio is 1 (no aerodynamic thrust), the dynamic center remains fixed in space and the oscillation takes place about this point. When the payload is 10,000 lb, the location of the point in space relative to the dynamic center about which the oscillation takes place can be found from the expression

$$Z_{IC} = -\left(\frac{1}{\omega_\theta^2}\frac{M'_y}{M'_x}Z_A\right)$$

which gives, with payload,

$$Z_{IC} = 62.7 \text{ ft}$$

indicating that the instant center (IC) of the longitudinal oscillatory mode is 62.7 ft above the dynamic center, a point 3.75 ft above the hull envelope.

A similar expression can be obtained for the lateral oscillatory mode.

$$Z^*_{IC} = -\left[(1/\omega_\phi^2)Z_A\right], \qquad Z^*_{IC} \cong 1.97 \text{ ft}$$

Thus the instant center of the lateral oscillatory mode is approximately 2 ft above the lateral dynamic center, i.e., 9.4 ft below the centerline of the hull.

Vehicle Response Characteristics

In this section, the response of these vehicles to step inputs in various controls is compared. The vehicle response characteristics are illustrated for a number of cases with payload and no control mixing. Various control inputs are employed. Recall that translational motion of the dynamic center is shown in the time histories presented. Figure 6 compares the response of the three configurations to a 1-deg collective pitch step input on all rotors. The vertical velocity increases slowly toward its ultimate steady-state value of about 14 ft/s. Inclusion of hull drag would reduce the steady-state vertical velocity as shown in Fig. 4 but have little impact on the rise time. Pitching motion is excited in all configurations since a moment is produced about the dynamic center. This motion is lightly damped for all configurations. Recall that on the birotor there is no way to reduce or control this pitching motion near hover, and, although small, may prove to be an annoyance in piloting the craft. External disturbances will also excite pitching motion. For the birotor, locating the rotors at the vehicle dynamic center would minimize the pitching motion due to control inputs but would result in a nonzero pitch attitude in steady flight. For the other configurations, gearing the controls would reduce the initial pitching motion. The pitching motion also produces a small translational velocity through the tilting of the aerodynamic thrust vector.

The vertical velocity response at zero payload will exhibit longer time constants due to reduction in vertical damping and control sensitivity.

Figure 7 shows the response to longitudinal cyclic pitch with payload. The primary response is a low level of translational acceleration with a small pitch motion induced by the location of the rotors below the dynamic center.

The cyclic responses are not shown for zero payload since no control is available in the case of the birotor and trirotor configurations. For the quadrotor vehicle, the response shown can be directly scaled to the response at any payload depending upon the assumption made regarding the maximum negative value of the thrust allowed for the rotor in sustained negative thrust operation.

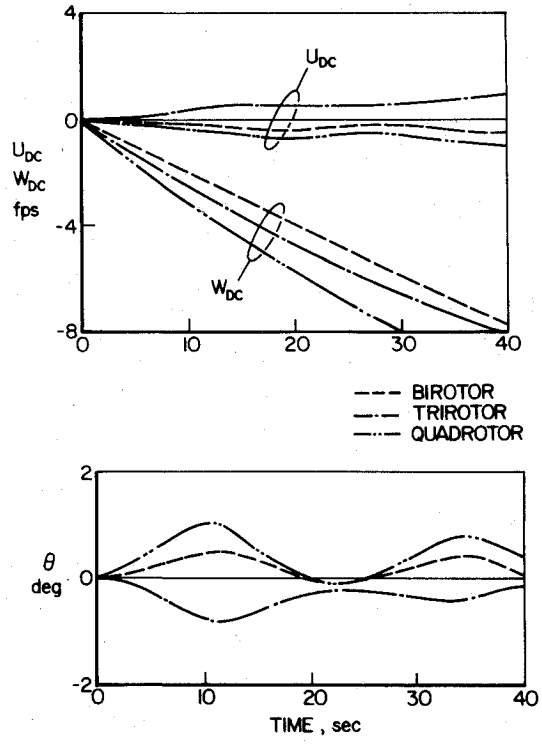

Fig. 6 Comparison of the longitudinal response of the three configurations to 1-deg collective step input on all rotors ($\beta = 0.85$).

Figures 8 and 9 show lateral-directional responses of the three configurations. The response to lateral cyclic on all rotors is shown in Fig. 8. A steady lateral acceleration is produced along with excitation of the lightly damped roll mode and a small yaw acceleration.

Different methods are available for yaw control, except for the birotor configuration, where only fore and aft cyclic of opposite sign on the two rotors produces a yawing moment. The control moment available will be directly proportional to the level of aerodynamic thrust, i.e., the vehicle buoyancy ratio. The yaw damping is negligible, therefore, a control input produces a constant yaw acceleration as shown in Fig. 9. The same method of control applied to the quadrotor will result in the same response as for the birotor. If lateral cyclic is used on the quadrotor, proportioned to produce no side force (unequal trim thrust), the vehicle rotates about its dynamic center and the control effectiveness is reduced by about 85% based on a maximum cyclic of 1 deg. If the cyclics are applied equally on both rotors there will be a small side force and rolling moment produced giving rise to the response shown in Fig. 9. The vehicle rotates about a point about 16 ft ahead of the dynamic center and the initial rolling acceleration is a little larger than the yaw acceleration which could be disconcerting to the pilot.

The trirotor configuration offers more options with regard to lateral control. If lateral cyclic is applied at the rear rotor in addition to fore and aft cyclic on the forward rotors, the response shown in Fig. 9 results. The vehicles rotates about a point about 10 ft ahead of the dynamic center and a small roll acceleration to the left is induced due to the location of the tail rotor. Rotation about the dynamic center with no net side force can be obtained by addition of lateral cyclic at the main rotors of such a level to produce zero net side force. This would increase the yaw moment acting on the vehicle by about 25% but would also induce a relatively large initial roll acceleration which would be 40% larger than the yaw acceleration. If this latter method of control is used, it would appear desirable to use lateral differential collective mixing to cancel the initial roll moment such that only a yawing moment is applied to the vehicle. Only a small of collective mixing would be required, as the differential collective control is, relatively speaking, quite powerful. With this control mixing, the response would essentially be the same as in the birotor case as shown in Fig. 9 with an increased yaw acceleration capability about twice the level available from the birotor.

The yaw acceleration for the birotor and quadrotor vehicles is approximately 0.2 deg/s^2/ deg. Full application of cyclic pitch of 10 deg produces an acceleration that implies that it would take about 30 s to rotate the vehicle 90 deg.

Summary

It can be seen for the configurations studied that the natural dynamics are dominated by responses largely inertial in nature. That is, the vehicle acts much like a mass with forces and moments applied to it, the damping forces and moments are small, and, consequently, the controls result primarily in accelerations rather than rates as would be characteristics of a hovering helicopter. The shortest time constant that associated with vertical climb and this time constant is 30 s in the case of the quadrotor which has the largest heave damping. The angular responses are dominated by lightly damped oscillations with the spring provided by the DC/CB spacing.

Control moments available are very small. The roll acceleration available in the case of the quadrotor is about a factor of 10 smaller than that estimated for a tandem helicopter of similar size.[14] The pitch acceleration is about a factor of 100 lower than this large proposed tandem design and the yaw acceleration is about a factor of 500 smaller; therefore, the vehicles clearly cannot be compared to a helicopter to judge their maneuverability.

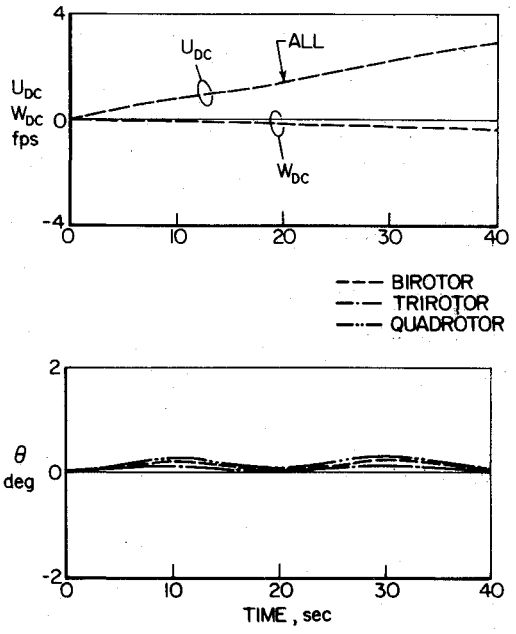

Fig. 7 Comparison of the longitudinal response of the three configurations to 1-deg longitudinal cyclic step input on all rotors ($\beta = 0.85$).

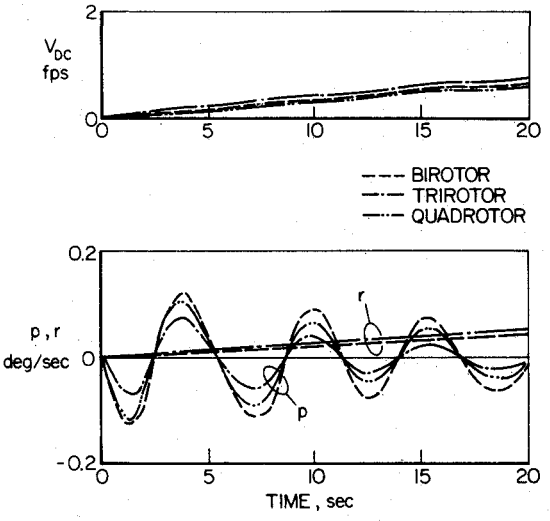

Fig. 8 Comparison of the lateral response of the three configurations to 1-deg lateral cyclic step input on all rotors ($\beta = 0.85$).

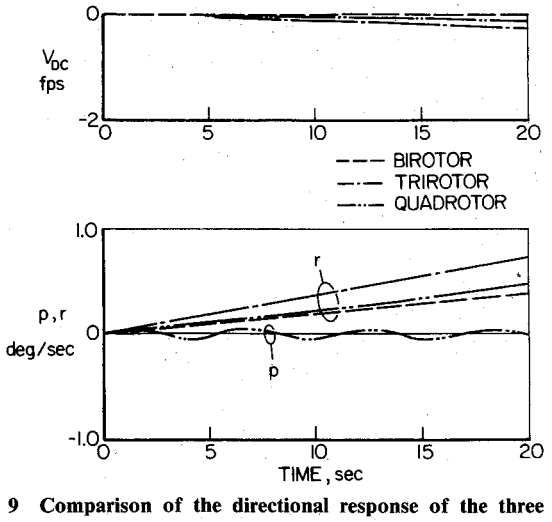

Fig. 9 Comparison of the directional response of the three configurations to 1-deg cyclic step input ($\beta = 0.85$).

Undoubtedly, the best way to control the vehicles is through direct force control, that is, with the use of the cyclic controls with mixing of differential collective to minimize angular motions. However, the control power available using this method of control is likely to be limited by allowable structural loads in the rotor blades and shaft.

The yaw axis response of these configurations in hover produces a similar response to that produced by equal angular rudder deflection on a conventional airship at a flight speed of 10-15 knots.

Conclusions

A study of the control characteristics and dynamic response characteristics of a conventional airship equipped with two, three, and four lifting rotors has shown the following.

1) All three configurations have similar response characteristics, characterized by relatively long time constants and lightly damped oscillatory modes in pitch and roll.

2) The lifting rotors provide small contributions to the vehicle angular damping. The magnitudes are similar to the level of damping provided by fixed tail surfaces at about a 10-knot flight speed.

3) Except in the case of the quadrotor, translational control forces are limited by buoyancy ratio.

4) A new approach to prediction of rotor characteristics at zero trim thrust in hover indicates that blade twist has a significant effect on the rotor thrust gradients with collective pitch and vertical velocity at low thrust coefficients.

5) To minimize angular motion of the vehicle with cyclic inputs, controls should be mixed such that zero moment is produced about the vehicle dynamic center.

6) Yaw control moments produced by cyclic pitch are equivalent to that produced by rudder deflection at 15 knots.

Appendix

Vehicle Parameters

Vehicle weight without payload: $W = 58{,}700$ lb
Buoyant force: $F_B = 58{,}700$ lb
Hull volume: $0.89 \times 10^6 \text{ft}^3$
Hull length: $L = 324$ ft
Maximum hull diameter: $D_m = 73.6$ ft
Added masses of hull: $M_{Ax} = 152$ slugs
$M_{Az} = M_{Ay} = 1889$ slugs
Tail added mass: $M_{AT} = 180$ slugs
Vehicle moments of inertia:

$$I_{xx_{CG}} = 0.448 \times 10^6 \text{ slug-ft}^2$$
$$I_{yy_{CG}} = 9.446 \times 10^6 \text{ slug-ft}^2$$
$$I_{zz_{CG}} = 9.446 \times 10^6 \text{ slug-ft}^2$$
$$I_{xz_{CG}} = -0.148 \times 10^6 \text{ slug-ft}^2$$

Added hull moment of inertia:

$$I_{A_{yy}} = I_{A_{zz}} = 7.550 \times 10^6 \text{ slug-ft}^2$$

Added tail moment of inertia:

$$I_{T_{xx}} = 0.212 \times 10^6 \text{ slug-ft}^2$$

Vehicle dimensions:

$$X_B = 0.0$$
$$Z_B = 24.0 \text{ ft}$$
$$\ell_T = 136.0 \text{ ft}$$

Rotor diameter: $D = 25.0$ ft
Number of blades per rotor: $b = 3$
Rotor solidity ratio: $\sigma = 0.089$
Blade lift-curve slope: $a = 5.73$ rad
Rotor angular velocity: $\Omega = 48.0$ rad/s
Transmission efficiency: $\eta_e = 0.92$
Figure of merit: $M = 0.65$
Blade effective twist: $\theta_l = -6.5$ deg

Acknowledgment

This research was supported by NASA Ames Grant NAG 2-98.

References

[1]Bailey, D. B. and Rappoport, H. K., "Maritime Patrol Airship Study (MPAS)," Naval Air Development Center, Warminster, Pa., NADC-80149-60, March 19, 1980.

[2]Bloetscher, F., Lancaster, J., and Faurote, G., "Feasibility Study of Modern Airships," NASA CR-137692, (Four volumes), Aug. 1975.

[3]Joner, B., Grant, D., Rosenstein, H., and Schneider, J. J., "Feasibility Study of Modern Airships," NASA CR-137 691 (Two volumes), May 1975.

[4]Curtiss, H. C. Jr. and Putman, W. F., "Stability and Control Characteristics of the Aerocrane Hybrid Heavy Lift Vehicle," *Journal of Aircraft,* Vol. 17, Oct. 1980, pp.

[5]Maisel, M., "Tilt Rotor Research Aircraft Familiarization Document," NASA TM X-62, 407, Jan. 1975.

[6]Tischler, M. B. et al., "Flight Dynamics Analyses and Simulation of Heavy Lift Airships," NASA CR 166471, 1981.

[7]Nagabhushan, B. L. and Tomlinson, N. P., "Flight Dynamics Simulation of a Heavy Lift Airship," *Journal of Aircraft,* Vol. 12, Feb. 1981, pp. 96-102.

[8]Tischler, M. B., Ringland, R. F., and Jex, H. R., "Heavy-Lift Airship Dynamics," *Journal of Aircraft,* Vol. 20, May 1983, pp. 425-433.

[9]Kochin, N. E., Kibel, I. A., and Roze, N. W., *Theoretical Hydrodynamics,* Interscience, New York, N.Y., 1964.

[10]Nielsen, J. H., *Missile Aerodynamics*, McGraw-Hill Book Co., New York, N.Y., 1960.

[11]Spangler, S. B. and Smith, C. A., "Theoretical Study of Hull-Rotor Aerodynamic Interference on Semibuoyant Vehicles," NASA CR 152127, April 1978.

[12]Seckel, E., *Stability and Control of Airplanes and Helicopters,* Academic Press, New York, N.Y., 1964.

[13]Strumf, A., "An Analysis of the Turning Characteristics of the XZP Airship Based Upon Underwater, Forced Turning Experiments," Davidson Laboratory, Hoboken, N.J., SIT-DL-54-534, Oct. 1954.

[14]Lytwyn, R. T. and Smith, R. P., "Analysis, Simulation, and Piloted Performance of Advanced Tandem-Rotor Helicopters in Hover," AHS Preprint 843, May 1974.